LAND USE/LAND COVER CLASSIFICATION AND SCALE EFFECT ANALYSIS FOR A MULTI-TEMPORAL SUPERPIXEL-BASED SEGMENTATION USING PLANETSCOPE DATA

Inacio T. Bueno[1,3], João F. G. Antunes[1,2], Ana P. S. G. D. Toro[3], João P. S. Werner[3], Rubens A. C. Lamparelli[1,3], Alexandre C. Coutinho[2], Gleyce K. D. A. Figueiredo[3], Júlio C. D. M. Esquerdo[2,3], and Paulo S. G. Magalhães[1]

[1]Interdisciplinary Center of Energy Planning, University of Campinas, Campinas 13083-896, SP, Brazil, ibueno@unicamp.br, lamparel@unicamp.br, graziano@unicamp.br;
[2]Embrapa Digital Agriculture, Brazilian Agricultural Research Corporation, Campinas 13083-886, SP, Brazil, joao.antunes@embrapa.br, alex.coutinho@embrapa.br, julio.esquerdo@embrapa.br; and
[3]School of Agricultural Engineering, University of Campinas, Campinas 13083-875, SP, Brazil, j164880@dac.unicamp.br, a265622@dac.unicamp.br, gleyce@unicamp.br.

ABSTRACT

Land-use land-cover (LULC) classification has long been an important topic in Earth observation research, frequently evaluated with recent advances in remote sensing science. This study evaluated the accuracy and suitability of LULC classifications based on the scale effect of a multi-temporal superpixel-based segmentation using PlanetScope (PS) data. We applied the Simple Non-Iterative Clustering (SNIC) algorithm testing five scale factors: 20, 50, 80, 110, and 140. We extracted statistical information of PS bands and vegetation indices from image-objects as input information for classification. In addition, segmentation tests were evaluated by analyzing the variability inside image-objects. Our results showed that the scale factor of 50 presented the highest accuracy while the scale factor of 20 returned the poorest. The scale factor of 20 also created a large number of image-objects inside land parcels, while scale factors of 110 and 140 merged adjacent areas. Segmentation evaluation demonstrated that a satisfactory scale factor for classification is essential once it directly affects the within-class variability and spoils segmentation suitability. The evaluation of these classifications has provided important insights into the effect of the scale factor in high-resolution imagery.

Key words — object-based image analysis, SNIC, scale factor, Google Earth Engine, Random Forest.

1. INTRODUCTION

LULC classification is a crucial planning tool illustrating the spatial distribution of the Earth's surface attributes and plays a pivotal role in the sustainable development of agronomics, environment, and economics [1].

In recent years, LULC classification procedures have been supported by the establishment of many satellites, new sensors, and the integration of advanced methods in digital image processing [2]. These new spaceborne platforms, such as the constellation of Planet CubeSats, have provided a powerful combination of high spatial (3 m pixel-size) and temporal (daily) resolution imagery for fine-scale LULC classification and monitoring [3].

Along with this growth in data availability, recent advances in digital image processing methods have improved the investigation of LULC classification accuracy. In particular, object-based image analysis (OBIA) has become more popular compared to traditional pixel-based classification methods due to their capability to delineate and classify the LULC at different scales [4].

Image segmentation is a crucial step in OBIA and divides an image into groups of pixels that are spatially continuous and spectrally homogeneous, also known as image-objects. In this regard, the SNIC algorithm [5], available in Google Earth Engine (GEE) [6], proved to be efficient in grouping a large number of pixels into smaller clusters called superpixels. Temporal information can also be included in the image segmentation step, called multitemporal segmentation. In this case, the segmentation output relies on spatial, spectral, and temporal attributes to delineate suitable objects affected by temporal dynamics [7].

In this study, we evaluated the accuracy of LULC classification based on the scale effect of a multi-temporal superpixel-based segmentation using PS data. In addition, we analyzed the image-objects variability and segmentation suitability while accounting for the influence of the scale factor parameter.

2. MATERIAL AND METHODS

2.1. Study area

The study area is located in the western region of São Paulo State, Brazil. Totaling 7,300 hectares, the area is occupied by LULC classes comprising cultivated pasture, eucalyptus plantations, native forest, integrated crop-livestock systems, shrub pasture, and wetlands.

2.2. PlanetScope data processing

We acquired PS images from September 1st 2017, to August 31st 2020, covering the study region. This time interval corresponds to the period of three agricultural years in the region: 2017-2018, 2018-2019, and 2019-2020. We selected all surface reflectance images with 0% of cloud cover to generate cloud-free time series for each agricultural year.

A set of nine PS band/indices was generated to classify the LULC in the study area: the Enhanced Vegetation Index (EVI), Green Normalized Difference Vegetation Index (GNDVI), Modified Soil Adjusted Vegetation Index (MSAVI), Normalized Difference Vegetation Index (NDVI), and Soil Adjusted Vegetation Index (SAVI). We also used PS spectral bands Blue, Green, Red, and NIR.

To overcome long image gaps in the time series due to cloud cover, we calculated a 10-day image composition by selecting the median value of each band/index in a 10-day interval. These image composites also provided a more consistent time series with equal time intervals.

2.3. Superpixel segmentation and parameter setting

Image superpixel multitemporal segmentation was implemented within the GEE environment based on the SNIC algorithm performed on the NDVI images of each agricultural year. This method created multitemporal image objects by segmenting multiple NDVI images of sequential periods. It incorporated spectral, spatial, and temporal information from NDVI images, which created objects based on the LULC dynamics in time, such as crop activities.

The multitemporal segmentation was based on two main steps. First, a grid of seeds established a superpixel seed location spacing (denoted hereafter by scale factor), influencing the image-objects size. This study tested five scale factors: 20, 50, 80, 110, and 140 PS pixels. These values were identified after some initial general experiments and considering the shape characteristics of the LULC classes in the study area. Second, SNIC required setting some main parameters: the "compactness factor" was set to 0.5 and affects the object shape; the "connectivity" was set to 4 and defined the type of contiguity to merge adjacent objects, and a "neighborhoodSize" was set to 256 to avoid tile boundary artifacts. We set these parameters considering the characteristics of the LULC classes and applied the same parameter configuration for all tests.

2.4. Reference data

Field campaigns were carried out from May 2019 and February 2020 to collect reference data points. The LULC information was collected based on the current land cover during the field campaigns and interviewing local farmers to obtain the area's historical land use. From the reference data, we set six LULC classes: cultivated pasture, eucalyptus plantations, native forest, integrated crop-livestock systems, shrub pasture, and wetlands.

2.5. LULC classification

From image-objects, we extracted four descriptive attributes: mean, 95th and 5th percentile (hereafter labeled as maximum and minimum respectively), and standard deviation based on each band/index values inside the objects. The initial pool of variables was screened to limit the potential effects of multicollinearity by calculating correlations between pairs of variables using the Pearson's R correlation coefficient. We removed those with R values greater than 0.90.

We used the Random Forest algorithm (RF; [8]) to classify the LULC in the study area. In this study, we tuned three RF parameters that control the structure of the algorithm: the number of trees to grow, or Ntree; the number of predictors sampled at each tree node, or Mtry; and the minimum size of terminal nodes. The control of node size parameter defines the minimum number of observations in a terminal node. We used the following parameter values in the RF tuning: Ntree = {200, 600, 1000}; Mtry = {$\sqrt{p}/4$, $\sqrt{p}/2$, $\sqrt{p}$} with p the total number of variables; and node size = {2, 6, 10}.

Five RF classifications, representing each scale factor test were performed. We balanced the number of observations by sampling 100 image-objects per LULC class when available, then split the data into 70% for training, while 30% was used for the test set to assess the generalization error of the RF model. Observations of training and test sets were sampled from the first two agricultural years (2017-2018 and 2018-2019) while all observations from the last year (2019-2020) were set for prediction analysis and LULC maps illustration. Finally, the overall accuracy of test sets, the total number of image-objects, and the number of image-objects per hectare were calculated in order to compare the performance of scale factor-based segmentations.

2.6. Segmentation evaluation

The segmentation tests were evaluated by analyzing the variability inside image-objects. The standard deviations by LULC class of the entire set of variables were graphically presented using boxplots. In addition, a qualitative analysis through visual interpretation of segmentation suitability was also done.

3. RESULTS

The overall accuracies based on segmentation tests allowed us to evaluate the performance of the scale factor parameter (Table 1). The superpixel-based segmentation test with a scale factor of 50 presented the highest overall accuracy, while the scale factor of 20 was the lowest. Another interesting aspect of these results is that the overall accuracy decreased once the scale factor increased after the test of 50.
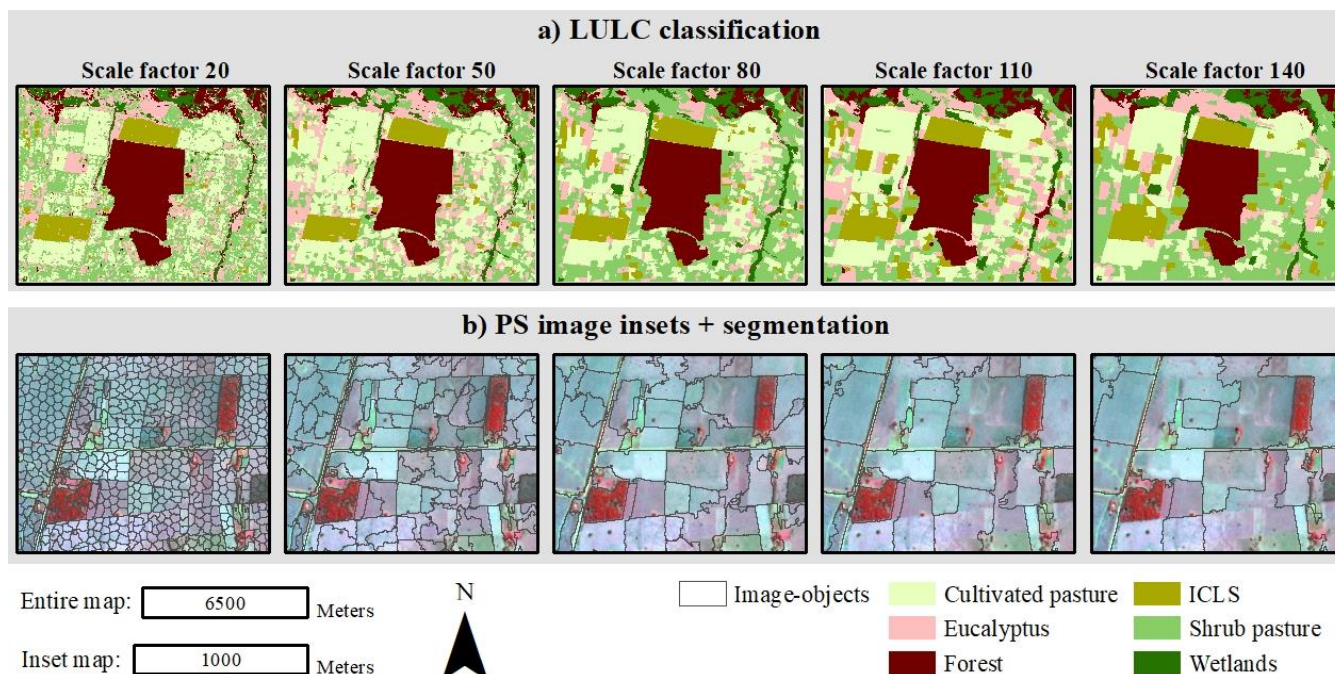
Figure 1. a) LULC classification maps based on each scale factor, and b) PS image in false color composite (R = NIR, G = Red, B = Green) with scale factor segmentations.

Since the scale factor controls the image-object size, our results confirm that the larger the scale factor the fewer the number of image objects, ergo, the smaller the rate of image-objects per hectare (Table 1).

Scale factor	Number of image-objects	Image-objects/ha	Overall accuracy
20	32227	4.23	0.85
50	5103	0.68	0.94
80	2039	0.27	0.88
110	1086	0.14	0.87
140	670	0.09	0.86

Table 1. Accuracy analysis and segmentation outputs per scale factor.

LULC classification maps illustrated the overall accuracy achieved for each segmentation test (Figure 1a). Our results showed that lower-scale factors returned isolated image-objects, characterizing a slight "salt-and-pepper" speckle in classification outputs. There is also an "optimal" scale factor with regard to the visual analysis of the land parcels delineation. While the scale factor of 20 created a large number of image-objects inside land parcels and scale factors of 110 and 140 merged adjacent areas, scale factors of 50 and 80 seemed to generate suitable segmentations for the study area (Figure 1b).

Turning now to the segmentation evaluation, the class-related standard deviations are graphically presented in Figure 2. The most interesting aspect of these results is that

the greater the scale factor, the higher the variability inside image-objects. Some LULC classes presented higher variability than others considering a fixed scale factor, e.g., some Wetlands image-objects with a scale factor of 140 presented the highest values of standard deviations of all LULC classes.

4. DISCUSSION

The fundamental assumption in OBIA is that image-objects derived through multi-temporal segmentation correspond to LULC elements at the surface with additional temporal information. However, the optimal delineation may not be possible in all instances, particularly in superpixel-based segmentation, where image-objects have related sizes due to their growth around the seed grid.

We demonstrated that classification accuracies of multi-temporal segmentation were related to the shapes of the SNIC superpixels, essentially their size. Overall accuracy outputs decreased gradually when image-objects size increased. One potential reason is that large image-objects merge different adjacent LULC patches (e.g., forest and shrub pasture). Therefore, this affects the intra-variability and class-based descriptive attributes of image-objects, introduced in this study as mean, maximum, minimum, and standard deviation, which increases the complexity and uncertainty in the classification analysis.

However, the smallest scale factor also presented low accuracy and a slight "salt-and-pepper" speckle. This result may be explained by the fact that the integration of spectral

signatures across a small number of pixels decreases the contrast among LULC classes due to an increase in within-class spectral variation.
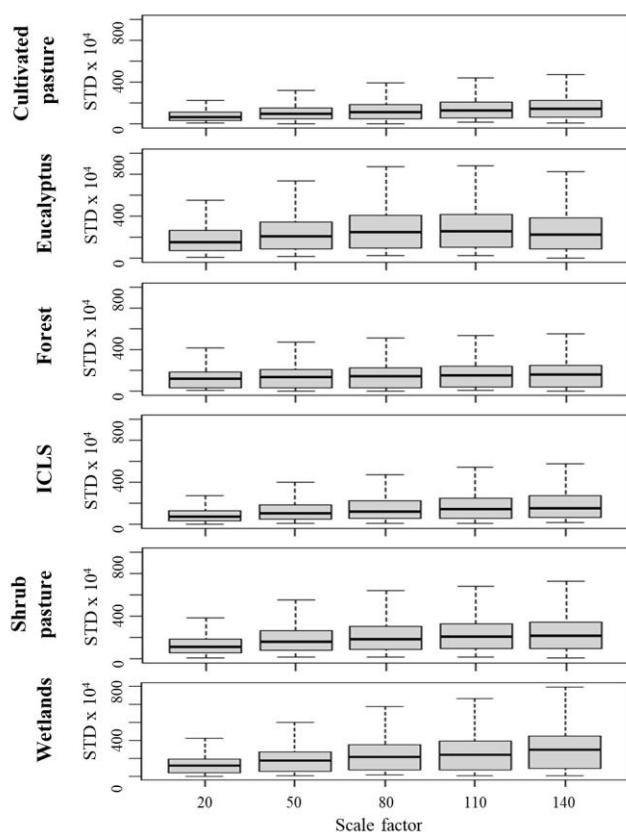

Figure 2. Band/index variability inside image-objects by LULC class and scale factor.

Based on our results, it can be determined that there is an evident scale effect in LULC classification using SNIC superpixel segmentation in PS images, which implied in the choice of an optimal scale factor for classification in our study area. This finding broadly supports the work of other studies about LULC classification linking scale factors with classification accuracies [9], [10]. However, specific scale analysis for specific objectives is essential, where not only the complexity of an image needs to be considered but also the feasibility of the method.

5. CONCLUSION

In this study, we have exploited the scale effect of a multi-temporal superpixel-based segmentation to evaluate the LULC classification accuracy in the western region of São Paulo State, Brazil. We demonstrated that there is an evident scale effect in classification accuracies using SNIC superpixel segmentation in PS images. The choice of a satisfactory scale factor for classification is essential once it

directly affects the within-class variability and spoils segmentation suitability. Thus, we encourage remote sensing scientists who require the highest quality of LULC classification to consider their choice of the scale factor carefully.

6. ACKNOWLEDGEMENTS

7. REFERENCES

[1] T. Václavík, S. Lautenbach, T. Kuemmerle, and R. Seppelt, "Mapping global land system archetypes," *Glob. Environ. Chang.*, vol. 23, no. 6, pp. 1637–1647, Dec. 2013, doi: 10.1016/J.GLOENVCHA.2013.09.004.

[2] C. Gómez, J. C. White, and M. A. Wulder, "Optical remotely sensed time series data for land cover classification: A review," 2016, doi: 10.1016/j.isprsjprs.2016.03.008.

[3] "Planet Imagery Product Specification." [Online]. Available: https://assets.planet.com/docs/Planet_Combined_ Imagery_Product_Specs_letter_screen.pdf.

[4] L. Ma, M. Li, X. Ma, L. Cheng, P. Du, and Y. Liu, "A review of supervised object-based land-cover image classification," *ISPRS J. Photogramm. Remote Sens.*, vol. 130, pp. 277–293, Aug. 2017, doi: 10.1016/j.isprsjprs.2017.06.001.

[5] R. Achanta and S. Süsstrunk, "Superpixels and polygons using simple non-iterative clustering," in *30th IEEE Conference on Computer Vision and Pattern Recognition*, 2017, pp. 4895–4904, doi: 10.1109/CVPR.2017.520.

[6] N. Gorelick, M. Hancher, M. Dixon, S. Ilyushchenko, D. Thau, and R. Moore, "Google Earth Engine: Planetary-scale geospatial analysis for everyone," *Remote Sens. Environ.*, vol. 202, pp. 18–27, Dec. 2017, doi: 10.1016/j.rse.2017.06.031.

[7] I. T. Bueno *et al.*, "Object-Based Change Detection in the Cerrado Biome Using Landsat Time Series," *Remote Sens.*, vol. 11, no. 5, p. 570, Mar. 2019, doi: 10.3390/rs11050570.

[8] L. Breiman, "Random forests," *Mach. Learn.*, vol. 45, no. 1, pp. 5–32, Oct. 2001, doi: 10.1023/A:1010933404324.

[9] X. Lv, D. Ming, Y. Chen, and M. Wang, "Very high resolution remote sensing image classification with SEEDS-CNN and scale effect analysis for superpixel CNN classification," *Int. J. Remote Sens.*, vol. 40, no. 2, pp. 506–531, Jan. 2019, doi: 10.1080/01431161.2018.1513666.

[10] N. B. Mishra and K. A. Crews, "Mapping vegetation morphology types in a dry savanna ecosystem: integrating hierarchical object-based image analysis with Random Forest," *Int. J. Remote Sens.*, vol. 35, no. 3, pp. 1175–1198, Feb. 2014, doi: 10.1080/01431161.2013.876120.